RESEARCH ARTICLE

Development and Characterization of Gingerol-Assisted Silver Nanoparticle and Chitosan Alginate Membrane for Antibacterial and Wound Healing Activity

Manisha Khaire, Papiya Bigoniya*

DSKM College of Pharmacy, Faculty of Pharmacy, RKDF University, Bhopal, Madhya Pradesh, India.

Received: 08th March, 2024; Revised: 26th May, 2024; Accepted: 02nd August, 2024; Available Online: 25th September, 2024

ABSTRACT

This study synthesized and characterized gingerol-loaded silver nanoparticles (Ag-NPs), which were incorporated into chitosan-alginate (Cs/Alg) films for advanced wound care applications. Gingerol was isolated with a 9.81% yield, forming pale-yellow needle-shaped crystals with a melting point of 32ºC. The purity and structure of gingerol were confirmed through thin-layer chromatography (TLC), UV-visible, fourier-transform infrared spectroscopy (FTIR), and high-performance liquid chromatography (HPLC) analyses. The synthesized Ag-NPs, particularly from the GN3 batch, exhibited a small particle size (36.52 ± 3.52 nm), high stability (zeta potential of -23.20 mV), and notable encapsulation efficiency (76.35%) and yield (74.11%). Scanning electron microscopy (SEM) and transmission electron microscopy (TEM) analyses revealed their spherical and smooth morphology. Stability tests over three months showed no substantial changes in particle size, ZP, or %EE. The Cs/Alg films demonstrated appropriate thickness, weight, water uptake, and pH changes, with GN-CM4 showing the best performance. *In-vitro* drug release studies indicated increased release rates, especially for GN-CM4, which also exhibited the highest antibacterial activity. *In-vivo* studies on excision and burn wound models showed that GN-CM4 promoted complete wound closure by day 21, enhanced hydroxyproline levels, reduced myeloperoxidase content, and facilitated superior tissue regeneration. These findings underscore the potential of gingerol-loaded Ag-NPs in enhancing wound healing through their anti-inflammatory and antibacterial properties.

Keywords: Gingerol, Silver nanoparticles, Chitosan alginate (Cs/Alg) film, Infected incision wound, Burn wound, wound healing

International Journal of Drug Delivery Technology (2024); DOI: 10.25258/ijddt.14.3.29

How to cite this article: Khaire M, Bigoniya P. Development and Characterization of Gingerol-Assisted Silver Nanoparticle and Chitosan Alginate Membrane for Antibacterial and Wound Healing Activity. International Journal of Drug Delivery Technology. 2024;14(3):1456-1468.

Source of support: Nil.

Conflict of interest: None

INTRODUCTION

Wound management is a critical aspect of healthcare, particularly in the context of increasing bacterial resistance and the demand for effective, biocompatible, and multifunctional wound dressings.[1] Traditional wound dressings frequently fail to prevent bacterial infections and promote rapid healing, highlighting the need for advanced therapeutic solutions. Naturally occurring phytoconstituents are well-documented for their potent antioxidant, anti-inflammatory, and antimicrobial properties, making it ideal candidates for enhancing wound healing. However, their therapeutic potentials are often limited by various factors, including solubility, permeation, and bioavailability.[2]

Recent advancements in nanotechnology, particularly the use of silver nanoparticles (Ag-NPs), have demonstrated significant ability in refining the antimicrobial efficacy and delivery of bioactive compounds because of their unique properties, for example, higher surface area, higher porosity, better penetration capability, and strong antibacterial and antioxidant capabilities. These nanoparticles enhance wound healing by influencing collagen deposition skin regeneration and providing resistance against microbial contamination.[1-3] Chitosan, derived from chitin, is highly valued for its pharmaceutical and tissue engineering as well as its role in accelerating wound healing by supporting tissue organization and promoting cell proliferation. When combined with alginate, which forms gels and enables painless dressing removal, these materials create highly effective wound dressings. The chitosan/alginate polyelectrolyte complex, formed through covalent and ionic crosslinking, enhances wound care and drug delivery by maintaining a moist environment that facilitates granulation and re-epithelialization. The integration of these

*Author for Correspondence: p_bigoniya2@hotmail.com

biopolymers into wound dressings ensures biocompatibility, biodegradability, and excellent film-forming properties, all of which contribute to a more efficient wound-healing process.[4,5]

Zingiber officinale, or ginger, is a widely used spice and medicinal plant with a wider range of therapeutic usage. Owing to its anti-inflammatory, antibacterial, and antioxidant qualities all of which aid in the healing of wounds, it has been traditionally utilized in many cultures. Among the many bioactive substances found in ginger are gingerols, which are the main aromatic compounds and, in particular, 6-gingerol, which has strong anti-inflammatory and antioxidant properties. Gingerols undergo drying or heating to become shogaols, which are likewise highly anti-inflammatory and antioxidant. One of the main sesquiterpenes in ginger essential oil, gingiberene, is responsible for some of its antibacterial properties. Furthermore, another class of bioactive substances found in ginger, called paradols has strong anti-inflammatory and antioxidant properties.[7-9]

Among the many ways that ginger promotes wound healing are its anti-inflammatory qualities, which lessen inflammation by preventing the fabrication of pro-inflammatory cytokines and enzymes like TNF-α and COX-2, which are essential for reducing the inflammatory phase and speeding up remodeling and proliferation. With substances like gingerols and shogaols shielding cells from oxidative damage, their antioxidant properties aid in scavenging free radicals, lowering oxidative stress, and encouraging cell proliferation and tissue regeneration.[10] The wide-ranging antibacterial properties of ginger inhibit the growth of bacteria and fungus, hence averting wound infections and fostering a sterile healing milieu. Additionally, it increases the synthesis of collagen, which helps with wound contraction and closure.[10]

Additionally, it may encourage angiogenesis, which is necessary to provide healing tissue with nutrition and oxygen. Uses include topical products like gels, ointments, and lotions; dressings infused with ginger to keep wounds moist and release bioactive chemicals in a controlled manner; and dietary supplements that offer systemic antioxidant and anti-inflammatory properties. Studies on animals have shown that wounds treated with ginger extract heal more quickly than those left untreated. These studies have also shown that ginger extracts can hinder the growth of bacteria, stimulate the proliferation of fibroblasts, develop the production of collagen *in-vitro*, and speed up wound contraction, re-epithelialization, and tensile strength *in-vivo*.[10,11]

Recent research has explored the potential of silver nanoparticles (Ag-NPs) combined with natural polymers for wound healing applications. Hydrogels composed of alginate, gelatin, and Ag-NPs demonstrated improved wound healing *in-vivo*, with enhanced granulation tissue development.[12] Chitosan-stabilized Ag-NPs exhibited multifunctional properties, including antibacterial, antifungal, and wound healing activities.[13] A chitosan-based film containing Ag-NPs showed superior wound closure rates compared to commercial products in animal studies.[14] Additionally, a bilayer dressing combining Ag-NPs loaded in metal-organic frameworks with chitosan nanoparticles and a polyvinyl alcohol/sodium alginate/chitosan layer established exceptional antibacterial activity as well as enhanced wound healing through reduced inflammation.[15] These studies highlight the potential of AgNP-based composite materials as effective wound dressings, offering antimicrobial protection and promoting tissue regeneration.[15]

Recent studies reveal that 10% ginger extract ointment significantly accelerates incision wound healing in rats. The phenolic compounds in ginger possess strong anti-inflammatory and wound-healing properties, with methanolic extract reducing edema by 98.3% and enhancing tissue repair in burn wounds.[16,17] ginger's antimicrobial efficacy is attributed to its volatile oil, gingerol, and other pungent principles, which inhibit prostaglandin and leukotriene production.[18] The plant's essential oil, rich in compounds like α-Zingiberene and β-sesquiphellandrene, demonstrates marked antimicrobial activities. These findings suggest potential applications for ginger in the pharmaceutical and food industries, though further research is needed to elucidate the underlying molecular mechanisms.[16-18]

Despite the potential of green-synthesized gingerol-assisted silver nanoparticles (Ag-NPs) embedded in chitosan for synergistic antibacterial effects, such formulations are currently lacking. This study seeks to fill that gap by isolating and characterizing bioactive phytoconstituents from plants known for their wound healing and antibacterial properties. This investigation aims to create and characterize a novel gingerol-assisted Ag-NP chitosan-alginate membrane, leveraging the combined therapeutic benefits of gingerol, silver nanoparticles, and biopolymer-based dressings. This study explores the antibacterial and wound-healing properties of innovative dressings, addressing gaps in current practices and supporting the development of more effective wound-healing solutions.

MATERIALS AND METHODS

Materials

Dried Indian ginger was sourced from Pune, Maharashtra. All solvents for extraction were procured from Loba Chemicals, AR grade. The water bath for setting various temperatures was acquired from Remi Instruments, Mumbai, India. Solvents used in HPLC and GC analyses were obtained from Spectrochem. Standards of 6-gingerol and zingerone were purchased from Sigma-Aldrich, India Ltd.

Methods

Plant preparation, extraction, and phytochemical analysis

Ginger (Zingiber officinale Rosc) rhizomes were collected and dried, followed by grinding to produce coarse powder. The dried material was then extracted with 96% ethanol (AR grade) at 70°C utilizing the soxhlet extraction method for 24 hours. The solvent was evaporated through distillation to yield a thick, pasty crude gingerol extract. This extract was suspended in water, initiating the ginger resin to precipitate,

which was subsequently detached through filtration. The resulting residue was dried underneath a vacuum to obtain gingerol, and the yield was calculated.[19]

Characterization of Gingerol

Organoleptic properties

The organoleptic properties were assessed visually by observing the appearance and the color.[19]

Melting point (MP)

The MP of the phytocompound was estimated with the Capillary technique and a Thiele tube melting apparatus. A glass capillary tube filled with powder was sealed, tied to a thermometer, and occupied in a heated Thiele tube with liquid paraffin. The melting point was documented, with the process repetitive thrice for accuracy.[20]

Preparation of stock solution

To create a calibration curve for phytoconstituents, a UV-vis spectrophotometer (JASCO V-530, Japan) was utilized. For the calibration of gingerol, 10 mg of the extract was dissolved in 20 mL of methanol within a 100 mL volumetric flask. The solution was then diluted up to the 100 mL mark with methanol, resulting in a final concentration of 100 µg/mL.[20]

Preparation of calibration curve

Various sample solutions (10–50 µg/mL) were prepared by diluting appropriate volumes of the stock solution with solvent in 10 mL volumetric flasks. The absorbance of all the dilutions was measured for maximum absorption wavelength utilizing a spectrophotometer on 200 to 400 nm wavelengths. The graph of absorbance versus concentration of phyto-components was plotted and analyzed for regression coefficient.[20]

Thin layer chromatography (TLC)

To prepare the TLC plate, silica gel-G slurry in distilled water was spread on 20 cm glass plates, forming a 0.25 to 0.30 mm thick layer. The plates were activated at 105°C for 1-hour. The sample was applied with a capillary 2 cm from the bottom and air-dried. A solvent system of hexane and diethyl ether (30:70) was used for gingerol. The mobile phase was added to the TLC chamber, capped, and saturated for 30 minutes. The spotted plates were then developed, examined visually and under UV light after applying a visualizing agent, and the RF value was estimated utilizing the formula:

Rf = Distance traveled by solute/Distance traveled by solvent ----- (1)[21]

Fourier-transform infrared spectroscopy (FTIR)

The FTIR examination was executed utilizing JASCO-460 plus an FTIR spectrophotometer (Japan). The samples were scanned in the range of 4000 to 400 cm^{-1} and The FTIR spectrum of gingerol was compared with the standard spectrum.[22]

High-performance liquid chromatography (HPLC)

Samples were analyzed utilizing HPLC with an Inertsil ODS-SP C18 column (250 × 4.6 mm, 5 µm) and an SPD-20A UV detector. The mobile phase was acetonitrile and water (55:45) with a flow rate of 1.3 mL/min. Detection was at 280 nm with a 10 µL injection volume. For sample preparation, 40 mg of gingerol was dissolved in HPLC-grade methanol and diluted to 25 mL. The instrument was configured according to the specified chromatographic conditions, a 10 µL sample was injected, and the chromatogram was recorded.[23]

Green synthesis of gingerol Ag-NP

Different concentrations of gingerol were mixed with 99 mL of 10 mM aqueous $AgNO_3$ in a round-bottom flask and stirred at 85°C for 3 hours. A color change from light yellow to reddish brown indicated nanoparticle formation. Afterward, the reaction was stopped, and the mixture was centrifuged at 9000 rpm. Pure Ag-NPs were isolated by repeated washing with distilled water. Four batches of gingerol Ag-NPs were formulated with gingerol concentrations of 1, 2, 5 and 10 mg/mL, designated as GN1, GN2, GN3, and GN4, respectively.[24]

Characterization of gingerol Ag-NP

Zeta potential (ZP) and Mean Particle size (MPS)

The MPS and ZP of the gingerol Ag-NPs were evaluated utilizing a Zetasizer Nano ZS (Malvern Instruments, UK). For determination of zeta potential, nanoparticulate formulations were diluted with 0.1 mL of water and then samples were analyzed in an electrophoretic cell.[25]

Entrapment efficiency (%EE)

The gingerol Ag-NPs formulations were subjected to ultracentrifugation at 10,000 rpm for 30 minutes and separated from the seeding solution. The pellets so obtained were dissolved in distilled water. The gingerol concentration was estimated from the supernatant solution utilizing UV spectrophotometry. The subsequent equation was used in the direction of calculating the %EE of gingerol

% EE = Experimental gingerol content / Theoretical gingerol content × 100 ---------- (2).[26]

Scanning electron microscopy (SEM)

The SEM of the synthesized nanoparticles was studied utilizing SEM (JEOL JSM-6360A, Singapore). The nanoparticles were uniformly spread on a glass slide (10 mm) and dried overnight at RT in a vacuum desiccator. These dried nanoparticles were used for SEM analysis and, mounted on solid support and coated with gold at an approximate thickness of 100 Å. The coated nanoparticles were examined under SEM and operated at 15 kV and images were captured at different locations.[27]

Transmission electron microscopy (TEM)

TEM (JEOL-JEM 2100) study was also utilized to study the morphology of the nanoparticles. Nanoparticulate suspension was spread on a carbon-coated copper grid and air-dried. The images were captured at an operating voltage of 120 kV.[28]

Stability of nanoparticle

The stability study of the optimized nanoparticles was performed for 3 months at 4°C in the stability chamber. The

samples were withdrawn at 1, 2 and 3M time points and particle size, ZP, %EE and appearance were determined and compared with initial observations.[28]

Gingerol chitosan/Alginate (CS/Alg) membrane

The solvent casting evaporation method was utilized to formulate the CS/Alg polyelectrolyte membranes. Activated low molecular weight alginate was prepared following a previously established method. Subsequently, a 3% chitosan solution was prepared utilizing 2% glacial acetic acid. This chitosan solution was then mixed with the activated alginate in various molar ratios, specifically 4:1, 3:1, 2:1, and 1:1. The mixture was stirred at 1,000 rpm for 30 minutes at room temperature, followed by pH adjustment to 5.5 utilizing HCl. The viscosity was measured at 100 rpm utilizing a Brookfield Viscometer at 25°C. Each of the four solutions then received 0.2 mL of G-Ag-NP solution, which was added during stirring to achieve complete homogeneity. Afterward, the solutions were deaerated, poured onto a glass plate, as well as permitted in the direction of drying at room temperature. The crosslinked chitosan/alginate membranes were subsequently washed with methanol and vacuum-dried at 40°C for 5 hours. The resulting gingerol Ag-NP-loaded membranes were labeled GN-CM1, GN-CM2, GN-CM3, and GN-CM4.[27,28]

Characterization of Gingerol Chitosan/Alginate (CS/Alg) membrane

Membrane thickness

Film thickness was estimated utilizing an Elcometer 456 coating thickness gauge in both dry and wet states. Measurements were recorded at various locations on the sample before and after wetting, with intervals of 15 minutes, 1, 3, 8, and 24 hours.[29]

Membrane weight and uniformity of mass

Twenty pieces of film, each measuring 2.5 × 2.5 cm, were cut from various areas of the film. The average mass of these pieces, along with the standard deviation (SD), was determined utilizing an analytical scale (GR-202, A&D Company Ltd., India). The %deviation from the average mass was then assessed.[29]

Water uptake capability

Each film was weighed three times and then equilibrated in 15 mL of PBS (pH 7.4) at room temperature for 24 hours. After equilibration, the films were blotted to remove excessive water and re-weighed. This process was repetitive while waiting for a constant weight to be achieved. The percentage of water uptake was then calculated:

Percent water uptake = [(WW-DW)/DW] × 100 ------ (3).[30]
Where, DW: Dry Weight; WW: Wet Weight

Drug content

A 10 mm diameter film from each batch was dissolved in 100 mL isotonic phosphate buffer (pH 6.8) for 6 hours with occasional stirring. Five ml of the solution was diluted with 20 mL of the same buffer, filtered through Whatman paper (0.45 mm), and the drug content was measured using a UV-visible spectrophotometer (JASCO V-530, Japan).[31]

%gingerol content = Experimental gingerol content / Theoretical gingerol content × 100 -----(4).

Membrane surface pH

The surface pH of the films was measured using a contact pH meter. A drop of purified water was applied to each film, and pH readings were taken at intervals over 24 hours, with each sample measured thrice.[32]

In-vitro drug release

In-vitro drug release was examined utilizing a Franz diffusion cell. Gingerol-loaded Cs/Alg membranes (1×1 cm) were positioned on a cellulose acetate membrane. The receptor compartment was filled with PBS at pH 7.4 and maintained at room temperature. Over a 24-hour period, samples were collected and analyzed utilizing UV spectrophotometry at 282 nm. To ensure sink conditions, fresh PBS was added to the receptor compartment following each sample collection.[33]

Antibacterial activity

The antibacterial activity of the gingerol Cs/Alg membrane was assessed utilizing the agar diffusion technique. Suspensions of *Aspergillus niger, Escherichia coli, Pseudomonas aeruginosa*, and *Staphylococcus aureus*, each with a final concentration of 10^8 cfu/mL (McFarland scale), were evenly spread on the surface of petri dishes containing Mueller-Hinton agar utilizing a cotton swab. After air-drying the agar for 5 minutes, 6 mm diameter membrane disks were placed on the swabbed agar and incubated overnight at 37°C. Antibacterial activity was assessed by measuring the inhibition zones around the disks. The experiments were done in triplicate.[34,35]

Wound Healing Activity

Experimental animals

In the animal study, Wistar albino rats (200–240 g, 12–16 weeks) were acclimatized for one week before experimentation. They were housed under controlled conditions (24 ± 2°C, 50 ± 5% RH) with a 12-hour light-dark cycle and provided with water and a standard diet. The study was performed as per ethical guidelines of the CPCSEA (CPCSEA Registration No: 1988/PO/Re/S/17/CPCSEA) and approved by IAEC (Approval No: GIPER/IAEC/22/06).[36]

Infected excision wound

On the day of wound creation, 36 rats were randomly distributed into six groups: Group 1 (wound control), group 2 (infected wound control), group 3 (sham Ag-NPs), group 4 (GN-3), group 5 (sham CS/Alg membranes), and group 6 (gingerol GN-CM4). The rats were anesthetized with ketamine (80 mg/kg, IP) and diazepam (5 mg/kg, IP) before wounds were created on their dorsal thoracic region, 1-cm from the vertebral column, utilizing a scalpel and scissors. After achieving hemostasis, the wounds were left exposed. On day 14, the

excised skin was collected for histological and biochemical analysis. All wounds, except those in the wound control group, were inoculated with *S. aureus* (1×10^6 CFU/mL). Treatment began on day 3, with the control groups receiving 0.9% saline. Groups 3 and 4 were treated daily with Ag-NPs, while groups 5 and 6 were treated with pre-moistened chitosan-alginate films. These films were covered with gauze and tape and were replaced on days 4, 7, 14, and 21 after hydration with saline and light anesthesia.[36]

Burn wound

Thirty experimental animals were divided into five groups: Group 1 (burn wound control), group 2 (sham Ag-NPs), group 3 (GN-3), group 4 (sham CS/Alg membranes), and group 5 (gingerol GN-CM4). A deep burn wound, 15 mm in diameter and 177 mm^2 in area was created on the dorsal surface utilizing an electrical heater at 110°C for 10 seconds, followed by cleaning the skin with normal saline. Treatment started 24 hours post-wounding, designated as day 1. The burn wound control group was treated with 150 µL of 0.9% saline and covered with gauze and tape. Groups 2 and 3 received daily applications of a silver nanoparticle formulation and were left uncovered. groups 4 and 5 were treated with pre-moistened chitosan-alginate films (2 cm in diameter) utilizing 100 µL of 0.9% saline, with all wounds enclosed in gauze and tape. These treatments were adjusted daily with saline hydration until the 7th follow-up day, with films replaced on days 4, 7, 14, and 21 under light anesthesia. Burned skin was collected on day 14 for histological and biochemical analysis. Wound healing was assessed by measuring wound area, contraction, epithelialization period, myeloperoxidase and hydroxyproline levels and examining skin histology in both burn and excision wound models.[36]

Wound area

The wound area was assessed by tracing the wound onto translucent paper, which was then placed on a 1-mm^2 graph sheet for measurement on days 1, 4, 7, 14, and 21, and subsequently every other day until the wound was fully closed. Wound contraction was calculated as a percentage of the original wound size. Inflammatory features, for example, infiltration, edema, abscesses, lesions, and exudates, were evaluated every 48 hours.[36]

Wound contraction

Wound closure was assessed by tracing the wound on specific days utilizing transparent paper and a permanent marker. The traced areas were then measured with 1-mm^2 graph paper to determine the wound contraction rate and epithelialization period. The %wound contraction was calculated relative to the early wound size.[36]

%Wound closure = (WA on 1st day − WA on day (n) / WA on 1st day × 100 ---------- (5).

Where, n is the number of days (2nd, 4th, etc.) and WA: Wound Area

Epithelialization period

Complete epithelialization was defined by the detachment of the scab with no raw wound remaining. The number of days required for this to occur was recorded as the epithelialization period.[36]

Myeloperoxidase assay

Skin samples were stored in Eppendorf flasks containing an ice-cold buffer (0.1M NaCl, 20 mM NaPO4, 15 mM Na-EDTA, pH 4.7) at 28°C. Absorbance was measured at 450 nm utilizing a 96-well micro-plate reader, and the outcomes were reported as PMNs × 10^3 cells/mg of tissue, calibrated against a standard curve.[37]

Hydroxyproline content

Skin samples were incubated at 60°C for 15 hours, then homogenized with 6N hydrochloric acid and incubated at 130°C for 4 hours. After cooling and adjusting the pH to 7.0, hydroxyproline standards and samples were added to a 96-well plate. Chloramine-T and Ehrlich's reagent were added, and absorbance at 550 nm was measured to determine hydroxyproline concentration using a standard curve.[37]

Histological processing

Skin samples were fixed in 3.7% buffered formaldehyde (pH 7.4) for 24 hours, sectioned into 5 µm slices, and stained with hematoxylin and eosin (HE) for histological analysis of inflammatory infiltrate, blood vessels, and fibroblasts.[38-42]

RESULT AND DISCUSSION

Characterization of Isolated Gingerol

The physicochemical characterization of the isolated gingerol was performed. The yield was found to be 9.81%, which was colorless, odorless crystals with a melting point of approximately 32ºC. TLC analysis of gingerol revealed an RF value of 0.40. The maximum absorbance of gingerol was observed at 282 nm. The calibration curve demonstrated a linear correlation between absorbance and concentration, with a regression coefficient of 0.9964. FTIR spectra of gingerol displayed characteristic peaks at 3400 (OH), 1630.25 (C=O), and 1329.30 cm^{-1} (OH phenolic stretching). HPLC analysis, conducted as per the method reported by Mishra et al. (2013), showed a retention time (RT) of 4.2 minutes, corresponding to 4.3 minutes (Figures 1, 2, 3, and 4).

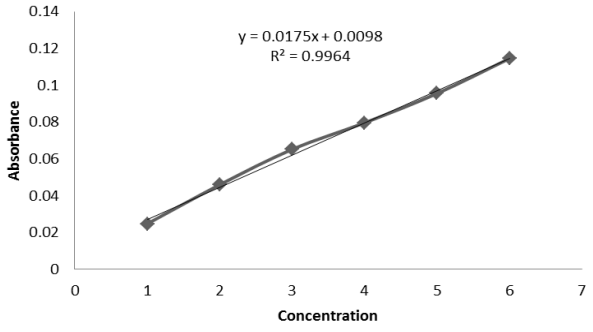

Figure 1: Calibration curve of gingerol

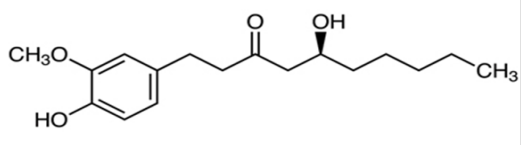

Figure 2: Chemical structure of gingerol

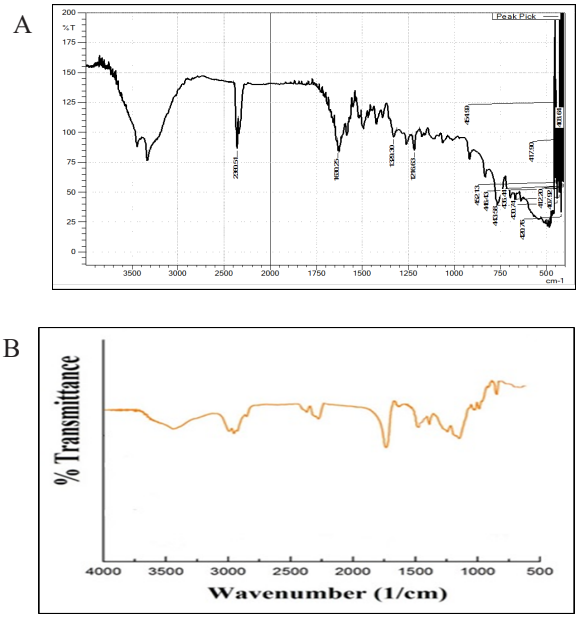

Figure 3: FTIR spectra of isolated gingerol (A) and reference gingerol (B) reported in (Singh *et al*., 2019)

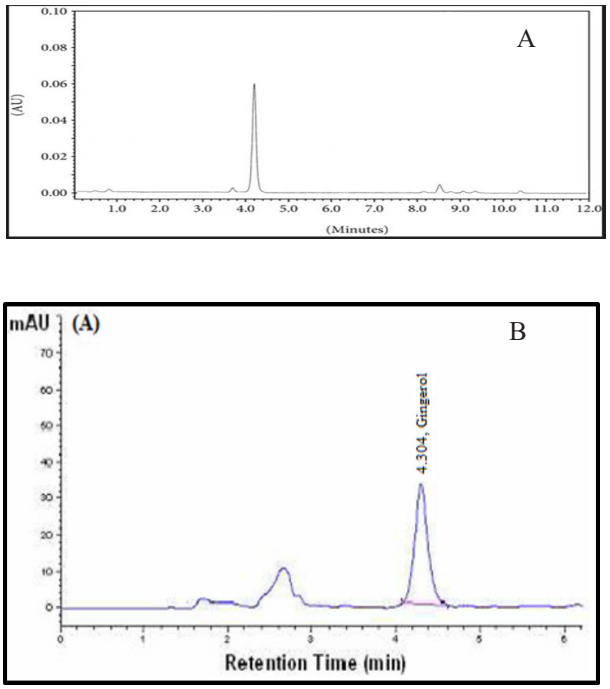

Figure 4: HPLC spectra of isolated gingerol (A) and standard gingerol (B) reported in Mishra *et al*. (2013)

Characterizations of gingerol Ag-NPs

Gingerol Ag-NPs were developed utilizing a green synthesis method, followed by thorough physicochemical characterization. The particle size of the nanoparticles varied between 36.52 nm for GN3 and 45.72 nm for GN1, indicating their potential for biological applications. Notably, the GN3 formulation had a significantly smaller average particle size of 36.52 ± 3.52 nm ($p < 0.01$) compared to the other formulations. Both GN3 and GN4 batches demonstrated a substantial increase in zeta potential, recorded at -23.20 and -27.16 mV, respectively, which implies enhanced electrical stability ($p < 0.001$). Furthermore, the GN3 batch exhibited a significantly higher gingerol entrapment efficiency of 76.35% and a product yield of 74.11% ($p < 0.01$–0.001). SEM investigation indicated that GN3 Ag-NPs were spherical with a smooth surface, while TEM images confirmed that these nanoparticles were uniformly sized, spherical, and non-aggregated (Table 1, Figures 5 and 6).

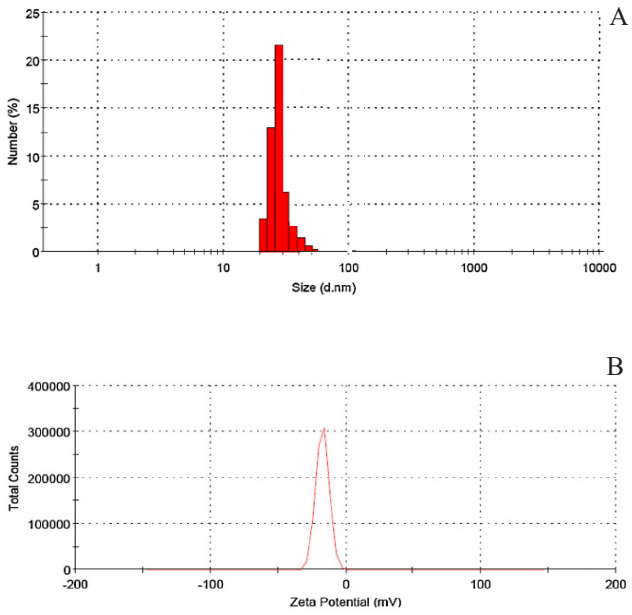

Figure 5: Particle density index (A) and zeta potential (B) of gingerol-loaded nanoparticle batch GN3

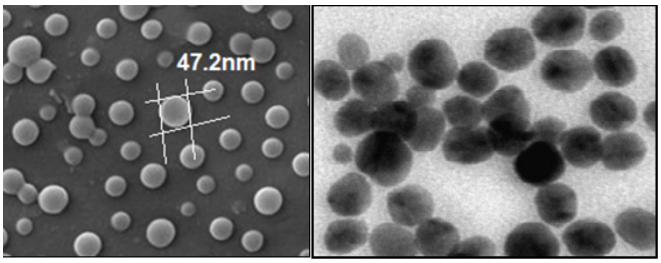

Figure 6: Scanning electron micrograph (A) and transmission electron microscopy (B) of gingerol-loaded silver nanoparticle batch GN3

Table 1: Characterizations of gingerol Ag-NP batches

Batch No	*Gingerol (mg/mL)*	*Yield (%)*	*Particle size (nm)*	*Zeta potential (mV)*	*Entrapment efficiency (%)*
GN1	01	67.63 ± 0.58	39.86 ± 2.40	-8.62 ± 0.34	69.51 ± 0.29
GN2	02	69.98 ± 0.61*	45.72 ± 4.17**	-20.38 ± 0.61***	72.30 ± 0.37*
GN3	05	74.11 ± 0.39***	36.52 ± 3.52^{ns}	-23.20 ± 0.28***	76.35 ± 0.48***
GN4	10	72.52 ± 0.16**	37.60 ± 3.62^{ns}	-27.16 ± 0.72***	74.82 ± 0.31**

1.Values are expressed as Mean ± SD for three observations (n = 3). ** $p < 0.01$, *** $p < 0.001$, and ns = not significant when compared to GN1 group values. 2. Values are expressed as Mean ± SD for 3 observations (n = 3). * $p < 0.05$, ** $p < 0.01$, *** $p < 0.001$, and ns = not significant when compared to GN1 group values.

Table 2: Stability study of optimized gingerol silver nanoparticle batch GN3

Storage time	*0 day*	*1 Month*	*2 Month*	*3 Month*
MPS (nm)	37.50 ± 0.17	37.60 ± 0.05^{ns}	37.60 ± 0.75^{ns}	37.50 ± 0.17^{ns}
ZP (mV)	-27.15 ± 0.31	-27.16 ± 0.65^{ns}	-27.15 ± 0.21^{ns}	-27.16 ± 0.35^{ns}
(%EE)	76.34 ± 0.15	76.34 ± 0.52^{ns}	76.35 ± 0.16^{ns}	76.35 ± 0.37^{ns}

Values are communicated as mean ± SD for 3 observations (n=3). ns = not significant when equated to the respective zero day values.

Table 3: Film thickness of gingerol chitosan alginate membrane batches

Batch No.	*Thickness (µm)*					
	Dry State	*15 Minutes*	*1 Hour*	*3 Hours*	*8 Hours*	*24 Hours*
Gingerol silver nanoparticle dressing						
GN-CM1	92.60 ± 2.48	154.34 ± 0.26***	175.61 ± 0.53***	235.73 ± 0.32***	257.84 ± 0.26***	388.53 ± 0.24***
GN-CM2	93.15 ± 3.73	236.68 ± 0.19***	238.48 ± 0.87**	256.28 ± 0.34***	257.85 ± 0.19**	408.22 ± 0.19***
GN-CM3	97.72 ± 3.16	198.19 ± 0.37***	240.90 ± 0.26***	289.80 ± 0.89***	380.42 ± 0.53***	467.30 ± 0.65***
GN-CM4	98.40 ± 4.54	188.52 ± 0.22***	197.27 ± 0.56***	198.34 ± 0.54^{ns}	289.90 ± 0.79***	335.25 ± 0.43***

Values are expressed as Mean ± SD for three observations (n = 3). *$p < 0.05$, ** $p < 0.01$,*** $p < 0.001$, and ns = insignificant when compared to the dry stat thickness of the film.

Stability of Gingerol Ag-NPs GN3

There were no significant changes in gingerol %EE, particle size and ZP of Ag-NPs batch GN3 over the storage period of three months (Table 2). Over a 3-month storage period, the particle size of the gingerol Ag-NPs remained stable, measuring approximately 37.50 nm, with minimal variation (37.60 ± 0.05–37.60 ± 0.75 nm). The ZP also remained consistent at around -27.15 to -27.16 mV, indicating stable electrical properties. Similarly, the (%EE) of gingerol was consistently high, ranging from 76.34 to 76.35%, with no significant changes observed over the storage period.

Characterization of Gingerol Cs/Alg Membrane

The thickness of all the films (GN-CM1–GN-CM4) in their dry state ranged between 92.60 and 98.40 µm. After wetting, the film thicknesses of all formulations increased significantly ($p < 0.001$) over a 15-minute to 24-hour period. The average weight of the prepared film samples ranged from 61.27 to 98.92 mg. Among these, formulation GN-CM4 demonstrated a significantly higher weight and drug content (98.06%) ($p < 0.001$). The water uptake capacity of all the preparations was similar, with GN-CM4 showing the highest absorption, attributed to its 1:1 chitosan-alginate ratio. The pH of all batches changed significantly over time, with GN-CM4 increasing from 2.22 to 5.98 after 24 hours (Table 3, 4, 5 and 6).

Drug Content Uniformity

In-vitro drug release

The GN-CM1 and GN-CM2 batches exhibited moderately significant increases in drug release throughout the first hour, monitored through a significantly higher release profile from the second to the 6 hours. In contrast, the GN-CM3 batch showed no significant change in drug release during the initial hour, but the release profile increased extremely significantly from the second hour through to the 6 hours. The GN-CM4 batch demonstrated an extremely significant increase in drug release throughout the entire 6 hours study (Table 7 and

Table 4: Film weight, water uptake and drug content of gingerol chitosan alginate membrane batches

Sample	*Avg. weight (mg)*	*Min weight (mg)*	*Max weight (mg)*
Gingerol silver nanoparticle dressing			
GN-CM1	66.27 ± 0.69	61.84 ± 0.43	72.20 ± 0.21
GN-CM2	91.61 ± 0.48***	87.37 ± 0.38***	98.83 ± 0.15***
GN-CM3	75.18 ± 0.23***	68.90 ± 0.17***	80.86 ± 0.87***
GN-CM4	94.80 ± 0.59**	89.73 ± 0.29***	98.92 ± 0.36***

Values are expressed as Mean ± SD for three observations (n = 3). * $p < 0.05$, ** $p < 0.01$, *** $p < 0.001$, and ns = not significant when compared to GN-CM1, GN-CM1 and CN-CM1 group values.

Table 5: Alteration of pH in gingerol chitosan alginate membrane batches

Batch No.	*pH*				
	After wetting	*pH alterations in determined time intervals*			
		15 Minutes	*1 Hour*	*3 Hours*	*8 Hours*	*24 Hours*
Gingerol silver nanoparticle dressing						
GN-CM1	2.17 ± 0.32	4.07 ± 0.64**	4.08 ± 0.61**	4.65 ± 0.36**	5.95 ± 0.16***	6.21 ± 0.19***
GN-CM2	2.17 ± 0.24	3.98 ± 0.35*	4.03 ± 0.23**	4.28 ± 0.47**	5.92 ± 0.66***	6.26 ± 0.46***
GN-CM3	2.11 ± 0.18	3.86 ± 0.47*	4.17 ± 0.41**	4.25 ± 0.61**	4.65 ± 0.58**	6.07 ± 0.15***
GN-CM4	2.22 ± 0.40	3.77 ± 0.12*	3.99 ± 0.24**	3.99 ± 0.15**	4.14 ± 0.46***	5.98 ± 0.23***

Values are expressed as Mean ± SD for 3 observations (n = 3). * $p < 0.05$, ** $p < 0.01$, ** $p < 0.001$, and ns = not significant when compared to initial wetting pH values.

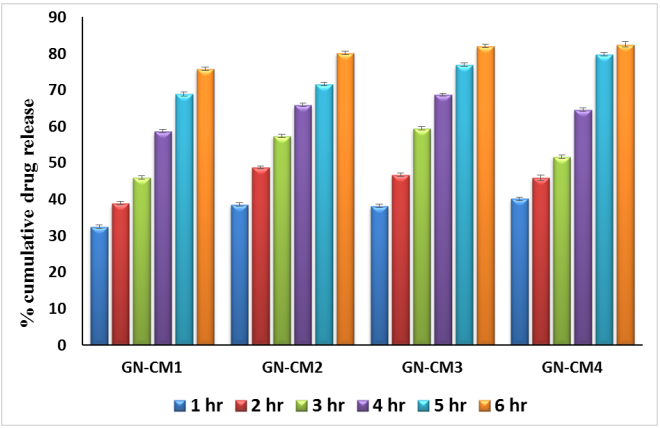

Figure 7: *In-vitro* drug release data of GN-CM1 – GN-CM4

Figure 7). The cumulative drug release from the gingerol-loaded membranes increased over time for all1 formulations. After 1 hour, the release ranged from 32.47 to 40.16%, with GN-CM4 showing the highest initial release. By 6 hours, release percentages had risen significantly, reaching 75.81% for GN-CM1 and up to 82.48% for GN-CM4. GN-CM3 exhibited the highest cumulative release at each time point, particularly notable at 5 hours with 76.88% and 6 hours with 81.99%. All formulations showed significant increases in drug release over time, with GN-CM4 achieving the highest cumulative release by the end of the 6-hour period.

Antimicrobial Activity

The antimicrobial activity of gingerol chitosan alginate membrane batches against four microorganisms was assessed. GN-CM1 showed inhibition zones of 3.06 ± 0.98 mm (*A. niger*), 13.12 ± 0.14 mm (*S. aureus*), 15.34 ± 1.12 mm (*P. aeruginosa*), and 1.09 ± 0.73 mm (*E. coli*). GN-CM2 had improved activity against *A. niger* (7.16 ± 1.78 mm, * $p < 0.05$) and *E. coli* (8.15 ± 0.66 mm, *** $p < 0.001$). GN-CM3 showed higher inhibition for *A. niger* (16.22 ± 0.59 mm, ** $p < 0.01$), *S. aureus* (16.38 ± 1.47 mm, ** $p < 0.01$), and *E. coli* (13.67 ± 0.78 mm, *** $p < 0.001$), but reduced for *P. aeruginosa* (1.89 ± 0.19 mm, *** $p < 0.001$). GN-CM4 exhibited enhanced inhibition for all microorganisms: *A. niger* (12.36 ± 1.09 mm, ** $p < 0.01$), *S. aureus* (17.51 ± 0.11 mm, ** $p < 0.01$), *P. aeruginosa* (7.25 ± 1.89 mm, ** $p < 0.01$), and *E. coli* (8.22 ± 0.89 mm, *** $p < 0.001$) (Table 8).

Table 6: Drug content uniformity in gingerol chitosan alginate membrane batches

Batch No.	*%Drug content*
GN-CM1	95.04 ± 0.46
GN-CM2	92.23 ± 0.19*
GN-CM3	96.81 ± 0.61ns
GN-CM4	98.06 ± 0.18*

Values are expressed as Mean ± SD for three observations (n = 3). * $p < 0.05$, ** $p < 0.01$, and ns = not significant when compared to GN-CM1, GN-CM1 and CN-CM1 group values.

Table 7: *In-vitro* diffusion of gingerol chitosan alginate membrane batches

Time in hr	*%cumulative drug release*			
	GN-CM1	*GN-CM2*	*GN-CM3*	*GN-CM4*
1	32.47 ± 0.43	38.55 ± 0.47	38.15 ± 0.48	40.16 ± 0.48
2	38.87 ± 0.46**	48.72 ± 0.46***	46.78 ± 0.50**	45.87 ± 0.76**
3	45.99 ± 0.44***	57.33 ± 0.45***	59.47 ± 0.47***	51.66 ± 0.49***
4	58.73 ± 0.48***	65.87 ± 0.47***	68.64 ± 0.39***	64.58 ± 0.45***
5	68.87 ± 0.50***	71.56 ± 0.48***	76.88 ± 0.49***	79.76 ± 0.47***
6	75.81 ± 0.44***	80.14 ± 0.48***	81.99 ± 0.46***	82.48 ± 0.73***

Values are expressed as Mean ± SD for three observations (n = 3). * $p < 0.05$, ** $p < 0.01$, *** $p < 0.001$, and ns = not significant when compared to 1-hour drug release values

Table 8: Antimicrobial activity of gingerol chitosan alginate membrane batches

Batch No	*Zone of inhibition (mm)*			
	A. niger	*S. aureus*	*P. aeruginosa*	*E. coli*
GN-CM1	3.06 ± 0.98	13.12 ± 0.14	15.34 ± 1.12	1.09 ± 0.73
GN-CM2	7.16 ± 1.78*	12.71 ± 1.14 ns	15.43 ± 1.03 ns	8.15 ± 0.66***
GN-CM3	16.22 ± 0.59**	16.38 ± 1.47**	1.89 ± 0.19***	13.67 ± 0.78***
GN-CM4	12.36 ± 1.09**	17.51 ± 0.11**	7.25 ± 1.89**	8.22 ± 0.89***

Values are expressed as mean ± SD for 3 observations (n = 3). * $p < 0.05$, ** $p < 0.01$, *** $p < 0.001$, and ns = not significant when compared to GN-CM1 group values respectively

Table 9: Effect of gingerol Ag-NP and chitosan alginate membrane on wound closure of infected excision in rats

Post-wounding days	*Wound area (mm²) and %wound contraction*					
	Wound control	*Infected wound*	*Silver nanoparticle*	*GN3*	*Chitosan alginate film*	*GN-CM4*
Day 0	311.94 ± 13.90	309.45 ± 12.12	312.93 ± 15.18	319.34 ± 14.42	315.21 ± 12.01	309.92 ± 13.13
	298.56 ± 14.28**	290.66 ± 12.67**	301.87 ± 12.11ns	309.15 ± 13.95*	302.48 ± 12.16**	290.74 ± 13.95**
Day 1	−4.69%	−6.07%	−3.53%	−3.19%	−4.03%	−6.18%
	286.42 ± 13.10***	524.26 ± 13.15***	442.91 ± 18.17***	219.11 ± 11.18***	412.66 ± 14.21***	218.52 ± 10.18***
Day 4	−8.18%	+69.57%	+41.53%	−31.35%	+30.92%	−29.49%
	261.62 ± 15.52***	568.33 ± 14.33***	273.73 ± 10.88***	121.63 ± 7.21***	329.33 ± 14.59**	120.71 ± 5.21***
Day 7	−16.13%	+83.65%	−12.52%	−61.91%	+4.48%	−61.05%
	215.44 ± 14.52****	399.75 ± 15.15****	122.56 ± 11.18****	68.12 ± 3.98****	265.66 ± 11.54***	67.92 ± 4.98****
Day 14	−30.93%	+29.18%	−60.83%	−78.66%	−15.72%	−78.08%
	12.89 ± 11.20****	247.66 ± 12.16****	93.56 ± 6.21****	22.98 ± 1.64****	125.21 ± 8.47***	7.64 ± 1.15****
Day 21	−95.86%	−18.67%	−70.10%	−92.80%	−60.27%	−95.81%
	00***	212.33 ± 10.54****	78.64 ± 4.14****	7.69 ± 0 .75****	109.65 ± 6.15***	00***
Day 22	100%	−31.38%	−74.86%	−97.59%	−65.21%	100%
	00***	191.33 ± 5.22****	51.34 ± 2.81****	00***	82.28 ± 2.95***	00***
Day 23	100%	−38.17%	−83.59%	100%	−73.89%	100%
Epithelialization period (day)	21.66 ± 0.98	32.50 ± 1.74	26.43 ± 2.62	23.83 ± 2.11	29.33 ± 1.30	21.43 ± 2.61

Values are expressed as Mean ± SD for 3 observations (n = 3). * $p < 0.05$, ** $p < 0.01$, *** $p < 0.001$, and ns = not significant when compared to wound control.

Excision Infected Wound

The study evaluated the effect of gingerol silver nanoparticles (Ag-NP) and chitosan alginate membranes on wound closure in rats with infected excisions, as shown in Table 9. Initial wound areas on day 0 were similar across groups, ranging from 309.45 ± 12.12 to 319.34 ± 14.42 mm². By day 1, all groups exhibited wound contraction, with the infected wound group showing a reduction of 6.07% (290.66 ± 12.67 mm², ** $p < 0.01$) and the GN-CM4 group showing a 6.18% reduction (290.74 ± 13.95 mm², ** $p < 0.01$).

On day 4, the infected wound area increased by 69.57% (524.26 ± 13.15 mm², *** $p < 0.001$), whereas significant wound contraction was observed in GN3 (31.35% reduction, 219.11 ± 11.18 mm², *** $p < 0.001$) and GN-CM4 (29.49% reduction, 218.52 ± 10.18 mm², *** $p < 0.001$). By day 7, the infected wound group showed an 83.65% increase (568.33 ± 14.33 mm², *** $p < 0.001$), while GN3 and GN-CM4 groups exhibited significant reductions of 61.91% (121.63 ± 7.21 mm², *** $p < 0.001$) and 61.05% (120.71 ± 5.21 mm², *** $p < 0.001$), respectively.

On Day 14, GN3 and GN-CM4 continued to show pronounced wound contraction (78.66 and 78.08%, respectively, *** $p < 0.001$), compared to the infected wound group's 29.18% increase (399.75 ± 15.15 mm², *** $p < 0.001$). By day 21, GN3 and GN-CM4 groups exhibited 92.80% (22.98 ± 1.64 mm², *** $p < 0.001$) and 95.81% (7.64 ± 1.15 mm², *** $p < 0.001$) reductions in wound area, respectively, compared to the 18.67% reduction in the infected wound group (247.66 ± 12.16 mm², *** $p < 0.001$). Complete wound closure (100%) was achieved in the control, GN3, and GN-CM4 groups by day 23, whereas the infected wound group showed a 38.17% reduction (191.33 ± 5.22 mm², *** $p < 0.001$).

The epithelialization period was shortest in the GN-CM4 group (21.43 ± 2.61 days), followed closely by the wound control (21.66 ± 0.98 days), indicating superior wound healing properties. Infected wounds took the longest to epithelialize (32.50 ± 1.74 days). Values are expressed as mean ± SD for six observations (n = 3). Statistically significant was assessed at * $p < 0.05$, ** $p < 0.01$, and *** $p < 0.001$ compared to day 0.

Burn Wound

The study inspected the effect of gingerol Ag-NP and chitosan alginate membranes on burn wound closure in rats as shown in Table 10. Initial wound areas on day 0 were comparable across groups, ranging from 209.98 ± 10.12 to 225.62 ± 10.13 mm². By day 1, the burn wound control, silver nanoparticle, and chitosan alginate film groups showed slight increases in wound area by 4.88, 4.24, and 2.55%, respectively, while GN3 and GN-CM4 groups exhibited slight reductions of 1.09 and 2.16% respectively.

On day 4, significant wound contraction was observed in all treated groups compared to the burn wound control, which reduced by 7.99% (193.19 ± 8.15 mm², ** $p < 0.01$). The silver nanoparticle, GN3, chitosan alginate film, and GN-CM4 groups showed substantial reductions of 42.04% (122.67 ± 6.17 mm², *** $p < 0.001$), 36.57% (139.11 ± 9.18 mm², *** $p < 0.001$), 39.90% (129.33 ± 8.59 mm², *** $p < 0.001$), and 50.87% (110.81 ± 8.21 mm², *** $p < 0.001$), respectively.

By day 7, the burn wound control group showed a 17.77%

Table 10: Effect of gingerol Ag-NP and chitosan alginate membrane on burn wound closure in rats

Post-wounding days	*Wound area (mm^2) and % of wound contraction*				
	Burn wound control	*Silver nanoparticle*	*GN3*	*Chitosan alginate film*	*GN-CM4*
Day 0	209.98 ± 10.12	212.63 ± 11.18	219.33 ± 9.42	215.21 ± 11.01	225.62 ± 10.13
Day 1	220.23 ± 12.67*	221.65 ± 12.11*	224.94 ± 10.95 ns	212.87 ± 12.16 ns	220.74 ± 9.95 ns
	+4.88%	+4.24%	+2.55%	–1.09%	–2.16%
Day 4	193.19 ± 8.15**	122.67 ± 6.17***	139.11 ± 9.18***	129.33 ± 8.59***	110.81 ± 8.21***
	–7.99%	–42.04%	–36.57%	–39.90%	–50.87%
Day 7	172.66 ± 7.64***	100.73 ± 5.88***	101.63 ± 6.21***	75.66 ± 5.54***	57.61 ± 3.98***
	–17.77%	–52.62%	–53.66%	–64.84%	–74.46%
Day 14	168.33 ± 6.33***	69.11 ± 2.18***	78.12 ± 5.98***	25.21 ± 2.47***	21.93 ± 1.64***
	–19.82%	–67.49%	–64.38%	–88.28%	–90.28%
Day 21	115.19 ± 6.15***	39.46 ± 1.30***	22.98 ± 1.64***	00***	00***
	–45.14%	–81.44%	–89.52%	100%	100%

Values are expressed as Mean ± SD for 3 observations (n = 3). * $p < 0.05$, ** $p < 0.01$, *** $p < 0.001$, and ns = not significant when compared to burn wound control values.

reduction in wound area (172.66 ± 7.64 mm², *** $p < 0.001$). In contrast, the silver nanoparticle group had a 52.62% reduction (100.73 ± 5.88 mm², *** $p < 0.001$), GN3 a 53.66% reduction (101.63 ± 6.21 mm², *** $p < 0.001$), chitosan alginate film a 64.84% reduction (75.66 ± 5.54 mm², *** $p < 0.001$), and GN-CM4 a 74.46% reduction (57.61 ± 3.98 mm², *** $p < 0.001$).

By day 14, wound contraction continued, with the burn wound control showing a 19.82% reduction (168.33 ± 6.33 mm², *** $p < 0.001$). The silver nanoparticle, GN3, chitosan alginate film, and GN-CM4 groups exhibited reductions of 67.49% (69.11 ± 3.18 mm², *** $p < 0.001$), 64.38% (78.12 ± 5.98 mm², *** $p < 0.001$), 88.28% (25.21 ± 2.47 mm², *** $p < 0.001$), and 90.28% (21.93 ± 1.64 mm², *** $p < 0.001$), respectively.

By day 21, the burn wound control group had a 45.14% reduction (115.19 ± 6.15 mm², *** $p < 0.001$). The silver nanoparticle and GN3 groups showed reductions of 81.44% (39.46 ± 2.30 mm², *** $p < 0.001$) and 89.52% (22.98 ± 1.64 mm², *** $p < 0.001$), respectively. Complete wound closure (100%) was observed in the chitosan alginate film and GN-CM4 groups by day 21. Values are expressed as mean ± SD for six observations (n = 3), with statistical significance assessed at * $p < 0.05$, ** $p < 0.01$, and *** $p < 0.001$ compared to day 0 values.

Table 11: Hydroxyproline content (HyP) and myeloperoxidase assay in an infected excision model

Infected excision model		
	Hydroxyproline (µg/100 mg of tissue)	*Myeloperoxidase (U/mL)*
Wound control	41.83 ± 2.37	75.29 ± 3.69
Infected wound	24.27 ± 1.99***	102.54 ± 1.78***
Silver nanoparticle	81.52 ± 3.06***	21.06 ± 2.11***
GN3	81.52 ± 2.19***	12.69 ± 0.84***
Chitosan alginate film	92.34 ± 3.37***	15.64 ± 2.12***
GN-CM4	87.04 ± 2.21***	8.91 ± 0.33***

Table 12: Hydroxyproline content (HyP) and myeloperoxidase assay in burn wound model

Burn Wound model		
	Hydroxyproline (µg/100 mg of tissue)	*Myeloperoxidase (U/mL)*
Burn wound	29.16 ± 1.40	115.13 ± 5.62
Silver nanoparticle	86.49 ± 3.11***	23.28 ± 1.43***
GN3	83.41 ± 2.07***	16.76 ± 1.89***
Chitosan alginate film	98.83 ± 4.14***	18.54 ± 1.11***
GN-CM4	84.77 ± 2.69***	11.42 ± 1.68***

Hydroxyproline content (HyP) and Myeloperoxidase assay

The study assessed hydroxyproline content and myeloperoxidase activity in an infected excision wound model to evaluate collagen synthesis and inflammation as shown in Table 11. The wound control group had hydroxyproline content of 41.83 ± 2.37 µg/100 mg of tissue and myeloperoxidase activity of 75.29 ± 3.69 U/mL, while the infected wound group showed significantly lower hydroxyproline (24.27 ± 1.99 µg/100 mg) and higher myeloperoxidase (102.54 ± 1.78 U/mL) levels, indicating impaired healing. Treatment with silver nanoparticles, GN3, chitosan alginate film, and GN-CM4 significantly increased hydroxyproline levels and reduced myeloperoxidase activity, with the chitosan alginate film (92.34 ± 3.37 µg/100 mg, 15.64 ± 2.12 U/mL) and GN-CM4 (87.04 ± 2.21 µg/100 mg, 8.91 ± 0.33 U/mL) groups showing the most improvement. These results suggest that the treatments, particularly chitosan alginate film and GN-CM4, enhance collagen synthesis and reduce inflammation, promoting better wound healing. Statistical significance was determined at ***

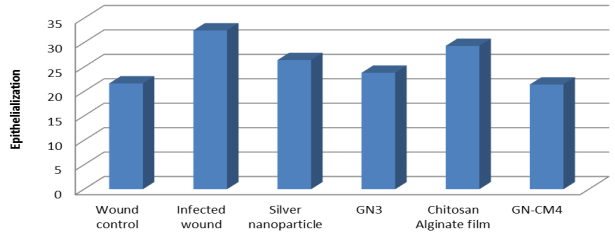

Figure 8: Effect of gingerol Ag-NP and chitosan alginate membrane on epithelization period of infected excision in rats

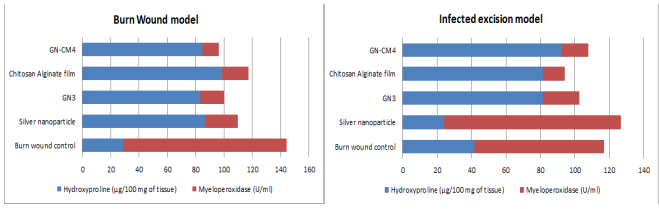

Figure 9: Effect of Gingerol Ag-NP and chitosan alginate membrane on hydroxyproline and myeloperoxidase content of infected excision and burn wound in rats

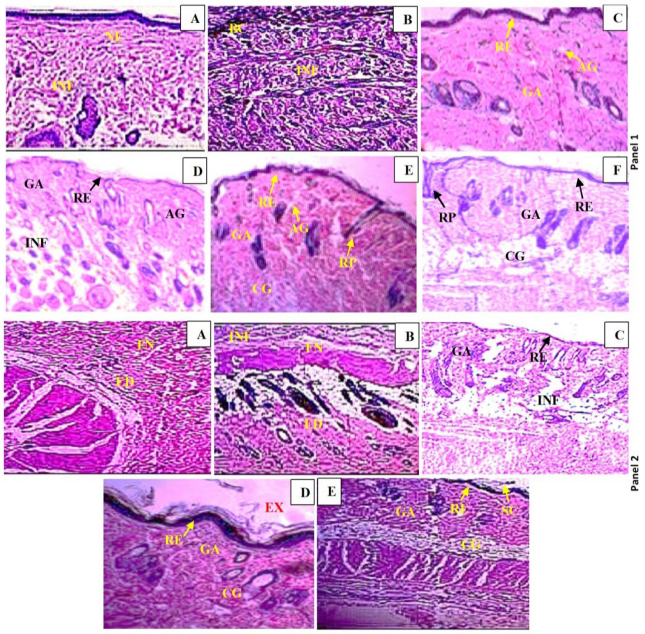

Figure 10: Histology of infected excision wound sections stained with hematoxylin and eosin. Epithelialization at wound control (A); Infected wound control (B); Silver nanoparticle (C); GN3 (D); Chitosan Alginate Film (E) and GN-CM4 (F) on 14th day (Panel 1). Histology of burn wound sections stained with hematoxylin and eosin. Epithelialization at wound control (A); Silver nanoparticle (B); GN3 (C); Chitosan Alginate Film (D) and GN-CM4 (E) on 14th day (Panel 2). AG (angiogenesis), BC (bacterial colonies), CG (collagen), ED (edema), EX (exudate), FN (fibrinoid necrosis), GA (granulation), INF (inflammation), NE (necrosis), RE (re-epithelization), RP (rete pegs) and SC (Scab).

$p < 0.001$ compared to the wound control group.

The study assessed hydroxyproline content and myeloperoxidase activity in a burn wound model to evaluate collagen synthesis and inflammation as shown in Table 12. The burn wound group exhibited low hydroxyproline content (29.16 ± 1.40 µg/100 mg of tissue) and high myeloperoxidase activity (115.13 ± 5.62 U/mL), indicating poor healing and significant inflammation. Treatment with silver nanoparticles, GN3, chitosan alginate film, and GN-CM4 significantly increased hydroxyproline levels and decreased myeloperoxidase activity. The chitosan alginate film group showed the highest hydroxyproline content (98.83 ± 4.14 µg/100 mg) and a notable reduction in myeloperoxidase activity (18.54 ± 1.11 U/mL), while GN-CM4 achieved substantial improvements with hydroxyproline at 84.77 ± 2.69 µg/100 mg and the lowest myeloperoxidase activity (11.42 ± 1.68 U/mL). These results suggest that the treatments, especially chitosan alginate film and GN-CM4, significantly enhance collagen synthesis and reduce inflammation, promoting better wound healing. Statistical significance was assessed at *** $p < 0.001$ compared to the burn wound group.

Figure 8: Impact of gingerol Ag-NP and chitosan-alginate membrane on the epithelization period of infected excision wounds in rats. Figure 9: Influence of gingerol Ag-NP and chitosan-alginate membrane on hydroxyproline and myeloperoxidase levels in infected excision and burn wounds in rats.

Wound Skin Histopathology

In the groups receiving gingerol Ag-NPs and chitosan-alginate films, tissue regeneration started at the wound edges, prominent in the direction of effective healing. In comparison, control and untreated wounds showed widespread bleeding and marked inflammation. The treated wounds developed a robust epidermal layer and dense granulation tissue, while untreated wounds had delayed re-epithelialization. Gingerol Ag-NP-treated wounds, in particular, demonstrated well-organized collagen fibers and substantial tissue regeneration with only minimal scabbing. Rats treated with gingerol Ag-NPs and chitosan-alginate films achieved complete re-epithelialization, evidenced by normal epidermal coverage and thicker, denser collagen fibers (Figure 10).

On the other hand, untreated rats suffered from persistent burn wounds with notable inflammation, necrotic tissue, and incomplete re-epithelialization. The sham-treated groups, including those with chitosan-alginate and gingerol-chitosan-alginate films, exhibited epidermal thickening, reduced presence of inflammatory cells, and extensive collagen deposition, along with significantly lower levels of neutrophil infiltration (Figure 10).

CONCLUSION

This research developed gingerol-loaded silver nanoparticles (Ag-NPs) incorporated into chitosan-alginate (Cs/Alg) films for wound care. Gingerol was isolated with a yield of 9.81% and characterized by TLC, UV-visible spectroscopy, FTIR, and HPLC. Ag-NPs, particularly the GN3 batch, exhibited a particle size of 36.52 ± 3.52 nm, high stability (zeta potential of -23.20 mV), and notable entrapment efficiency (76.35%). SEM

and TEM confirmed their spherical morphology. Cs/Alg films, especially GN-CM4, showed optimal performance in drug release and antibacterial activity. *In-vivo* studies demonstrated that GN-CM4 accelerated wound closure, enhanced tissue regeneration, and improved biochemical markers, highlighting its potential in wound healing applications.

REFERENCES

1. Rani Raju N, Silina E, Stupin V, Manturova N, Chidambaram SB, Achar RR. Multifunctional and Smart Wound Dressings—A Review on Recent Research Advancements in Skin Regenerative Medicine. Pharmaceutics. 2022 Jul 28;14(8):1574.
2. Oliveira A, Simões S, Ascenso A, Reis CP. Therapeutic advances in wound healing. Journal of Dermatological Treatment. 2022 Jan 2;33(1):2-2.
3. Ameen F, Srinivasan P, Selvankumar T, Kamala-Kannan S, Al Nadhari S, Almansob A, Dawoud T, Govarthanan M. Phytosynthesis of Ag-NP utilizing Mangifera indica flower extract as bioreductant and their broad-spectrum antibacterial activity. Bioorganic Chemistry. 2019 Jul 1;88:102970. DOI: https://doi.org/10.1016/j.bioorg.2019.102970
4. Bayda S, Adeel M, Tuccinardi T, Cordani M, Rizzolio F. The history of nanoscience and nanotechnology: from chemical–physical applications to nanomedicine. Molecules. 2019;25(1):112. DOI: https://doi.org/10.3390/molecules25010112
5. Bilgen F, Ural A, Kurutas EB, Bekerecioglu M. The effect of oxidative stress and Raftlin levels on wound healing. International wound journal. 2019;16(5):1178-1184. DOI: https://doi.org/10.1111/iwj.13177
6. Caetano GF, Frade MA, Andrade TA, Leite MN, Bueno CZ, Moraes ÂM, Ribeiro-Paes JT. Chitosan-alginate membranes accelerate wound healing. Journal of Biomedical Materials Research Part B: Applied Biomaterials. 2015;103(5):1013-1022. DOI: https://doi.org/10.1002/jbm.b.33277
7. Ali BH, Blunden G, Tanira MO, Nemmar A. Some phytochemical, pharmacological and toxicological properties of ginger (Zingiber officinale Roscoe): a review of recent research. Food and chemical Toxicology. 2008;46(2):409-420. DOI: https://doi.org/10.1016/j.fct.2007.09.085
8. Mao QQ, Xu XY, Cao SY, Gan RY, Corke H, Beta T, Li HB. Bioactive compounds and bioactivities of ginger (Zingiber officinale Roscoe). Foods. 2019;8(6):185. DOI: https://doi.org/10.3390/foods8060185
9. Shaukat MN, Nazir A, Fallico B. Ginger bioactives: A comprehensive review of health benefits and potential food applications. Antioxidants. 2023;12(11):2015. DOI: https://doi.org/10.3390/antiox12112015
10. Alharbi KS, Nadeem MS, Afzal O, Alzarea SI, Altamimi AS, Almalki WH, Mubeen B, Iftikhar S, Shah L, Kazmi I. Gingerol, a natural antioxidant, attenuates hyperglycemia and downstream complications. Metabolites. 2022;12(12):1274. DOI: https://doi.org/10.3390/metabo12121274
11. Bischoff-Kont I, Fürst R. Benefits of ginger and its constituent 6-shogaol in inhibiting inflammatory processes. Pharmaceuticals. 2021;14(6):571. DOI: https://doi.org/10.3390/ph14060571
12. Diniz FR, Maia RC, de Andrade LR, Andrade LN, Vinicius Chaud M, da Silva CF, Corrêa CB, de Albuquerque Junior RL, Pereira da Costa L, Shin SR, Hassan S. Silver nanoparticles-composing alginate/gelatine hydrogel improves wound healing *in-vivo*. Nanomaterials. 2020;10(2):390. DOI: https://doi.org/10.3390/nano10020390
13. Shehabeldine AM, Salem SS, Ali OM, Abd-Elsalam KA, Elkady FM, Hashem AH. Multifunctional silver nanoparticles based on chitosan: Antibacterial, antibiofilm, antifungal, antioxidant, and wound-healing activities. Journal of Fungi. 2022;8(6):612. DOI: https://doi.org/ 10.3390/jof8060612
14. Pansara C, Mishra R, Mehta T, Parikh A, Garg S. Formulation of chitosan stabilized silver nanoparticle-containing wound healing film: *in-vitro* and *in-vivo* characterization. Journal of pharmaceutical sciences. 2020;109(7):2196-2205. DOI:10.1016/j.xphs.2020.03.028
15. Zhang M, Wang G, Wang D, Zheng Y, Li Y, Meng W, Zhang X, Du F, Lee S. Ag@ MOF-loaded chitosan nanoparticle and polyvinyl alcohol/sodium alginate/chitosan bilayer dressing for wound healing applications. International Journal of Biological Macromolecules. 2021;175:481-494. DOI:10.1016/j.ijbiomac.2021.02.045
16. Jamaluddin AW, Lestari A. Effectiveness of ginger ointment (Zingiber officinale Roscoe) on incision wound healing in white rats (Rattus norvegicus). Jurnal Riset Veteriner Indonesia (Journal of The Indonesian Veterinary Research). 2021;5(1):20-26 DOI: https://doi.org/10.20956/jrvi.v5i1.13060
17. Bouchama C, Zinedine A, Rocha JM, Chadli N, El Ghadraoui L, Chabir R, Raoui SM, Errachidi F. Effect of phenolic compounds extracted from turmeric (Curcuma longa L.) and ginger (Zingiber officinale) on cutaneous wound healing in Wistar rats. Cosmetics. 2023;10(5):137. DOI:10.3390/cosmetics10050137
18. Aleem M, Khan MI, Shakshaz FA, Akbari N, Anwar D. Botany, phytochemistry and antimicrobial activity of ginger (Zingiber officinale): A review. The International Journal of Herbal Medicine. 2020;8(6):36-49. DOI:10.22271/flora.2020.v8.i6a.705
19. Khurana RK, Rao S, Beg S, Katare OP, Singh B. Systematic development and validation of a thin-layer densitometric bioanalytical method for estimation of gingerol employing analytical quality by design (AQbD) approach. Journal of Chromatographic Science. 2016;54(5):829-841. DOI: https://academic.oup.com/chromsci/article/54/5/829/1745060
20. Lwin OM, Giribabu N, Kilari EK, Salleh N. Topical administration of gingerol promotes healing of the wound of streptozotocin-nicotinamide-induced type-2 diabetic male rats. Journal of Dermatological Treatment. 2021;32(8):1039-1048. DOI: https://doi.org/10.1080/09546634.2020.1721419
21. Mahendran S, Badami S, Ravi S, Thippeswamy BS, Veerapur VP. Synthesis and evaluation of analgesic and anti-inflammatory activities of most active free radical scavenging derivatives of gingerol. British Journal of Applied Science & Technology. 2014;4(35):4959-4973. DOI: https://doi.org/10.9734/BJAST/2014/12745
22. Furniss BS, Hannaford AJ, Smith PWG, Tatchell AR. Vogel's, Textbook of Practical Organic Chemistry, 5th edition, Longman Scientific and Technical, England. 1989: 236-240. DOI: https://faculty.ksu.edu.sa/sites/default/files/vogel_-_practical_organic_chemistry_5th_edition.pdf
23. Biswas T, Sen A, Roy R, Maji S, Maji HS. Isolation of gingerol from flowering buds of Mangifera indica L and its evaluation of *in-vitro* antibacterial activity. Journal of Pharmaceutical Analysis. 2015;4(3):49-56. DOI: http://dx.doi.org/10.9755/ejfa.v26i7.18188
24. Meng X, Tian F, Yang J, He CN, Xing N, Li F. Chitosan and alginate polyelectrolyte complex membranes and their properties for wound dressing application. Journal of Materials Science:

Materials in Medicine. 2010;21:1751-1759. DOI: https://doi.org/10.1007/s10856-010-3996-6
25. Espinosa-Espinosa L, Garduño-Siciliano L, Rodriguez-Canales M, Hernandez-Portilla LB, Canales-Martinez MM, Rodriguez-Monroy MA. The wound-healing effect of mango peel extract on incision wounds in a murine model. Molecules. 2022;27(1):259. DOI: https://doi.org/10.3390/molecules27010259
26. Muruganandan S, Lal J, Gupta PK. Immunotherapeutic effects of gingerol mediated by the inhibition of oxidative stress to activated lymphocytes, neutrophils and macrophages. Toxicology. 2005;215(1-2):57-68. DOI: https://doi.org/10.1016/j.tox.2005.06.008
27. Nnamdi O. Development and characterization of mucoadhesive patches for buccal delivery of pregabalin. Universal Journal of Pharmaceutical Research. 2017;2(3):6-9. DOI: https://doi.org/10.22270/ujpr.v2i3.R2
28. Othman SN, Seka M. *In-vitro* antioxidant and cytotoxic activities of Ag-NP of gingerol isolated from Mangifera indica. Journal of Global Pharma Technology. 2019;11(6):10-15. DOI: http://www.jgpt.co.in/
29. Paul W, Sharma CP. Chitosan and alginate wound dressings: a short review. Trends in Biomaterials and Artificial Organs. 2004;18(1):18-23. DOI: https://tarjomefa.com/wp-content/uploads/2016/09/5300-English.pdf
30. Prajapati B, Raichandani Y, Patel R, Sawant K. Chitosan alginate film for topical drug delivery of antimicrobial agents. Current Pharmaceutical Research Journal. 2007;1(03):66-74. DOI: https://www.researchgate.net/publication/291116073_Chitosan_Alginate_Film_For_Topical_Drug_Delivery_Of_Antimicrobial_Agents
31. Rajendran P, Ekambaram G, Magesh V, Sakthisekaran D. Chemopreventive efficacy of gingerol against benzo (a) pyrene induced lung carcinogenesis in experimental animals. Environmental Toxicology and Pharmacology. 2008;26(3):278-282. DOI: https://doi.org/10.1016/j.etap.2008.05.005
32. Rasyid R, Ruslan R, Mawaddah S, Rivai H. Quantitative determination of gingerol in methanol extract of bacang mango (Mangifera foetida L.) leaves by thin-layer chromatography densitometry. World Journal of Pharmacy and Pharmaceutical Sciences.2020; 9(7):1551-1560. DOI: http://www.wjpps.com/
33. Samadarsi R, Dutta D. Design and characterization of gingerol nanoparticles for oral delivery. Journal of Food Engineering. 2019;247:80-94. DOI: https://doi.org/10.1016/j.jfoodeng.2018.11.020
34. Sharma S, Sanpui P, Chattopadhyay A, Ghosh SS. Fabrication of antibacterial silver nanoparticle—sodium alginate–chitosan composite films. RSC Advances. 2012;2(13):5837-5843. DOI: https://doi.org/10.1039/C2RA00006G
35. Sushanth KA, Lakshmi KC, Reddy DS. Evaluation of wound healing activity with a new formulation of dry Mangifera indica and honey utilizing swiss albino mice. Asian Journal of Pharmaceutical and Clinical Research. 2016:139-142. DOI: file:///C:/Users/admin/Downloads/admin,+Journal+manager,+AJPCR_11810_RA.pdf
36. Tenorová K, Masteiková R, Pavloková S, Kostelanská K, Bernatonienė J, Vetchý D. Formulation and evaluation of novel film wound dressing based on collagen/microfibrillated carboxymethylcellulose blend. Pharmaceutics. 2022;14(4):782. DOI: https://doi.org/10.3390/pharmaceutics14040782
37. Vandeputte OM, Kiendrebeogo M, Rasamiravaka T, Stevigny C, Duez P, Rajaonson S, Diallo B, Mol A, Baucher M, El Jaziri M. The flavanone naringenin reduces the production of quorum sensing-controlled virulence factors in Pseudomonas aeruginosa PAO1. Microbiology. 2011;157(7):2120-2132. DOI: https://doi.org/10.1099/mic.0.049338-0
38. Vyas A, Syeda K, Ahmad A, Padhye S, H Sarkar F. Perspectives on medicinal properties of gingerol. Mini Reviews in Medicinal Chemistry. 2012;12(5):412-425. DOI: https://doi.org/10.2174/138955712800493870
39. Kadhim O, Al-demirchi JY, Al-Hussainawy MK, Al-Hamdani MM, Kadhim AJ. Efficiency of Phenazine Compound Produced by Rhizospheric Pseudomonas fluorescens against Few Pathogenic Bacteria Isolated from Ear Infections. International Journal of Drug Delivery Technology. 2023;13(4):1167-1171. DOI: 10.25258/ijddt.13.4.07
40. Ismail WF, Al-Mudhafar MMJ, Fadhil AA, Synthesis, Characterization of New Isatin-Ibuprofen Derivatives with Expected Biological Activity. International Journal of Drug Delivery Technology. 2022;12(4):1560-1565. DOI: 10.25258/ijddt.12.4.13
41. Mohammed RH, Al-Niaame AE. Evaluation of the Biological Efficacy and Physicochemical Evaluation of Toothpaste Prepared from Few Types of Plant Extracts against Some Pathogenic Bacteria Isolated from the Mouth. International Journal of Drug Delivery Technology. 2022;12(4):1626-1631. DOI: 10.25258/ijddt.12.4.25
42. Mathew S, Sankarganesh P, Joseph B. Ecotoxicological Effects of Lead Exposed Cyprinus carpio and HSP70-Induced Antioxidants against ROS. International Journal of Drug Delivery Technology. 2023;13(4):1178-1182. DOI: 10.25258/ijddt.13.4.09